

Latitudinal transport of 7 MeV Jovian and galactic electrons

S. E. S. Ferreira¹, M. S. Potgieter¹, B. Heber², H. Fichtner³, and R. A. Burger¹

¹Unit for Space Physics, Potchefstroom University for CHE, 2520 Potchefstroom, South Africa.

²Fachbereich Physik, Universität Osnabrück, Barbarastrasse 7, 49069 Osnabrück, Germany.

³Institut für Theoretische Physik, Lehrstuhl IV: Weltraum- und Astrophysik, Ruhr-Universität Bochum, 44780

Abstract. The heliospheric modulation of galactic and Jovian electrons is studied using a fully three-dimensional, steady-state model based on Parker's transport equation including the Jovian source. The model is used to study the latitudinal transport of both 7 MeV Jovian and galactic electrons by illustrating how the electron intensities are affected at different latitudes when enhancing perpendicular diffusion in the polar directions. In particular, the electron intensity-time profile along the Ulysses trajectory is calculated for various assumptions for perpendicular diffusion in the polar directions and compared to the 3-10 MeV electron flux observed by Ulysses from launch up to the end of the first out-of-ecliptic orbit. Comparison of the model computations and the observations give an indication as to the magnitude of this diffusion coefficient. The relative contributions of the Jovian and galactic electrons to the total electron intensity are shown along the Ulysses trajectory.

the electron intensities at different latitudes are shown. In particular, the 7 MeV computed intensity-time profile along the Ulysses trajectory from launch up to the end of the first out of the ecliptic orbit is shown for different values of perpendicular diffusion in the polar region of the heliosphere. Compatibility between the model computations and the observed 3-10 MeV electron count rate (Heber et al., 2001) of the COSPIN/KET instrument onboard Ulysses gives an indication as to the magnitude of the perpendicular diffusion coefficient in the polar directions. For solutions compatible with observations the relative contributions of the Jovian and galactic electron intensity to the total computed intensity are shown in an attempt to distinguish between these two contributions.

1. Introduction

The Jovian magnetosphere at ~5 AU in the ecliptic plane is a relatively strong source of electrons with energies up to at least ~30 MeV (e.g. McDonald et al., 1972; Simpson et al., 1974; Teegarden et al., 1974). These Jovian electrons propagate along and across the heliospheric magnetic field (HMF), and are observed at Earth, and outward to ~30 AU (e.g., Eraker, 1982). The most recent measurements of a few-MeV electrons in the inner heliosphere (Ferrando et al., 1999; Heber et al. 2001) have been made with the cosmic ray and solar particle investigation (COSPIN) Kiel electron telescope (KET) (Simpson et al., 1992) onboard the Ulysses spacecraft. The Ulysses spacecraft has an orbit inclined by 80° and covers therefore a wide range of latitudes providing an excellent opportunity to study the latitudinal transport of ~7 MeV electrons in the inner heliosphere by comparing model results with the observations.

Using the three-dimensional model described below, a study is made of the latitudinal transport of 7 MeV electrons. The effects of various diffusion coefficients on

2. Modulation model and parameters

The model is based on a numerical solution of Parker's (1965) transport equation (TPE) :

$$\frac{\partial f}{\partial t} = -(\mathbf{V} + \langle \mathbf{v}_D \rangle) \cdot \nabla f + \nabla \cdot (\mathbf{K} \cdot \nabla f) + \frac{1}{3} (\nabla \cdot \mathbf{V}) \frac{\partial f}{\partial \ln P} + Q \quad (1)$$

where $f(\mathbf{r}, P, t)$ is the cosmic ray distribution function; P is rigidity, \mathbf{r} is position, and t is time. Terms on the right-hand side represent convection, gradient and curvature drifts, diffusion, adiabatic energy changes and the source function, respectively, with \mathbf{V} the solar wind velocity. The symmetric tensor \mathbf{K} consists of a parallel diffusion coefficient K_{\parallel} and two perpendicular diffusion coefficients, namely $K_{\perp r}$ the perpendicular diffusion coefficient in the radial/azimuthal direction and $K_{\perp \theta}$ the perpendicular diffusion coefficient in the polar directions. The anti-symmetric element K_A describes gradient and curvature drifts in the large scale HMF, with the averaged drift velocity \mathbf{v}_D . The source function Q , in this case for electrons produced at Jupiter, is given by:

$$Q = 1.5 \left(\frac{c_k j_{1.5} d_k j_{6.0}}{c_k j_{1.5} + d_k j_{6.0}} \right); j_{1.5} = 5 \times 10^3 E^{-1.5} \quad (2)$$

$$j_{6.0} = 10^9 E^{-6.0}; c_k = 0.6; d_k = 5.0$$

This function, with differential intensity j ($\text{m}^{-2}\text{sr}^{-1}\text{s}^{-1}\text{MeV}^{-1}$) and kinetic energy E (GeV), is a combination of $j \propto E^{-1.5}$

and $j \propto E^{-6.0}$ spectra, and is constructed to be compatible with normalized ISEE 3 (ICE) spectra (Moses, 1987), and Pioneer 10 data (Lopate, 1991) when Pioneer 10 was in or close to the Jovian magnetosphere. The source is treated as a point source (e.g., Pyle and Simpson, 1977) by specifying the source function in a single grid point in the code.

The TPE (1) was solved in a spherical coordinate system, with $\partial f/\partial t = 0$, that is a steady-state for solar minimum modulation with the current sheet "tilt angle" $\alpha = 15^\circ$ during so-called A > 0 epochs (~1990 to ~2001). The HMF was modified according to Jokipii and Kóta (1989) which is qualitatively supported by Ulysses measurements. The solar wind speed V was assumed to change from 400 km.s⁻¹ in the equatorial plane ($\theta = 90^\circ$) to a maximum of 800 km.s⁻¹ when $\theta > 60^\circ$ and $\theta < 120^\circ$. The outer boundary of the simulated heliosphere was set at 120 AU, where the electron spectrum of Langner et al. (2001) was used as the local interstellar spectrum (LIS) for galactic electrons. For the effects of other published LIS scenarios on model computations, see Ferreira et al. (SH 3.1.).

For K_{\parallel} , and the "drift" coefficient, K_A , the following general forms were assumed, respectively:

$$K_{\parallel} = K_0 \beta f_1(P, r); \quad K_A = (K_A)_0 \frac{\beta P}{3 B_m} \quad (3)$$

with

$$f_1(P, r) = \frac{1}{5} g(P) c(r) h(r, P);$$

$$h(r, P) = \frac{(P/P_0)^2 (r/r_0)^{1.7}}{50} + \frac{(P/P_0)(r/r_0)^{2.2}}{50} \quad (4)$$

$$+ 0.2(P/P_0)^{1/3} (r/r_0) + 7e(r); \quad \text{with:}$$

$$g(P) = \left(\frac{P_0}{P_s} \right)^{0.6}; \quad c(r) = \begin{cases} 1 & r > r_c \\ \frac{r_0}{r_c} \xi \left(\frac{r}{r_0} \right)^{\xi} & r \leq r_c \end{cases}$$

$$\xi = \left(\frac{r}{r_c} \right)^x; \quad x = \left(\frac{0.016}{P/P_0} \right)^{0.2};$$

$$r_c = \frac{r_0}{\frac{1}{10} + \left(\frac{P_s}{P_0} \right)^{1.4}}; \quad e(r) = \begin{cases} \frac{10 \text{ AU}}{r^k} & r > 10 \text{ AU} \\ 1 & r \leq 10 \text{ AU} \end{cases};$$

$$\text{with } k = \frac{(r/r_0)^2}{8000}.$$

Here, β is the ratio of the speed of the cosmic ray particles, v , to the speed of light; $f_1(P, r)$ is a function which gives the rigidity dependence P in GV, and the spatial dependence, with r the radial distance; $K_0 = 75.0$ is a constant in units of $6 \times 10^{20} \text{ cm}^2 \text{ s}^{-1}$; $(K_A)_0$ a dimensionless constant which specifies the amount of drifts allowed, with $(K_A)_0 = 1.0$ maximum; $P_0 = 1 \text{ GV}$, $r_0 = 1 \text{ AU}$, $P_s = P$ when $P < 1 \text{ GV}$ and $P_s = 1 \text{ GV}$ when $P \geq 1 \text{ GV}$. For the higher rigidities ($P > 0.1 \text{ GV}$), the parallel mean free path λ_{\parallel} is based on proton mean free path calculations by Burger et al. (2000), and for the lower rigidities ($P < 0.1 \text{ GV}$) λ_{\parallel} is compatible to calculations for the electron mean free path at Earth by Bieber et al. (1994) (see their Figure 10 for comparison) as well as electron mean free path observations at Earth (e.g., Bieber et al., 1994).

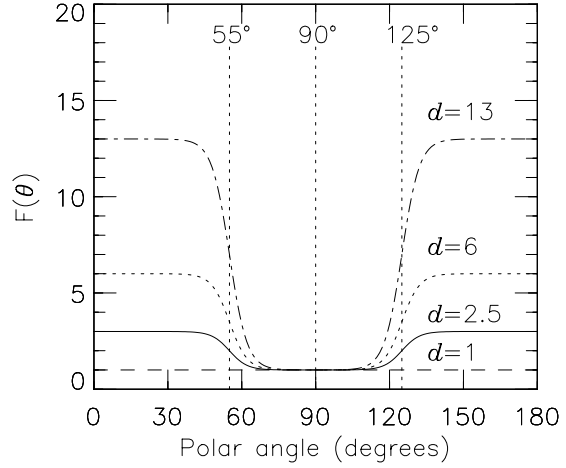


Fig. 1. $F(\theta)$, given by Eq. (6), as a function of polar angle for four different assumptions for d , which gives the magnitude increase in $F(\theta)$ towards the poles.

Unfortunately, no exact theory exists to adequately describe perpendicular diffusion (e.g. le Roux et al., 1999). It has become standard practice to scale K_{\perp} (meaning both $K_{\perp r}$ and $K_{\perp \theta}$) as K_{\parallel} (see e.g., Jokipii and Kóta, 1995; Potgieter, 1996; Ferreira et al., 2000 and Burger et al., 2000). However, the ratio K_{\perp}/K_{\parallel} is an extremely important parameter in modulation studies, especially at the lower energies where the effect of K_{\perp} on modulation becomes more important than K_{\parallel} (Ferreira et al., 2000). Here, $K_{\perp \theta}/K_{\parallel} = 0.020$ (Ferreira et al., 2001a) in the equatorial plane, and $K_{\perp r}/K_{\parallel} = 0.005$ at 7 MeV for all polar angles (Ferreira et al., 2001b).

Kóta and Jokipii (1995) revived the concept that K_{\perp} might be anisotropic and that it should be larger in the polar directions than in the radial direction. Therefore, it has also become standard practice to increase the value of K_{\perp} in the polar directions (e.g., Kóta and Jokipii, 1995; Potgieter, 1996; Burger et al., 2000; Ferreira et al., 2000; Ferreira et al., 2001a) illustrated that in order to produce the correct magnitude and rigidity dependence of the observed latitudinal cosmic ray proton gradient by Ulysses, enhanced latitudinal transport is required. This is accomplished by increasing $K_{\perp \theta}$ towards the poles with respect to the equatorial plane by assuming

$$K_{\perp \theta}/K_{\parallel} = bF(\theta) \quad (5)$$

with $b = 0.020$. The function $F(\theta)$ is given by

$$F(\theta) = A^+ + A^- \tanh\left[\frac{1}{\Delta\theta}(\theta_A - 90^\circ + \theta_F)\right] \quad (6)$$

with $A^{\pm} = (d \pm 1)/2$, $\Delta\theta = 1/8$, $\theta_A = \theta$ and $\theta_F = 35^\circ$ for $\theta \leq 90^\circ$ while for $\theta > 90^\circ$, $\theta_A = 180^\circ - \theta$ and $\theta_F = -35^\circ$. According to Eq. (6), $K_{\perp \theta}$ is enhanced with respect to K_{\parallel} by a factor d , that is from the value b in the equatorial regions towards the poles.

Equation (6) is shown in Fig. 1 as a function of polar angle with four different values for d of which the subsequent effects on the modulation will be shown below. Figure 1 illustrates how $F(\theta)$ increases from unity towards the poles depending on the value for d .

3. Results and discussion

To establish what the magnitude of the factor increase in $K_{\perp\theta}$ towards the polar regions should be, the model computations are compared to 3-10 MeV electron measurements by Ulysses. In Fig. 2 the effects on modulation for the computed 7 MeV electron intensities are shown along the Ulysses trajectory for the four values of d . In comparison, the 3-10 MeV (~ 7 MeV) 4-day averaged electron count rate of the COSPIN/KET instrument onboard Ulysses is shown. The top gray line, with the selection of "1 electron" event (Ferrando et al., 1996), and the bottom gray line corrected for the estimated γ -ray background (Heber et al., 2001) are considered as upper and lower limits respectively. The trajectory of the Ulysses spacecraft (e.g., Heber et al., 2001) is shown in the two top panels in terms of the radial distance from the Sun, and its heliographic latitudinal position θ_{lat} for selected time periods. The second panel shows the relative contribution of the galactic and Jovian electron intensities to the computed total intensity. The third panel shows the 7 MeV computed Jovian intensity only, and the fourth panel the computed 7 MeV galactic electron intensity only. The fifth panel shows the combined Jovian and galactic electron intensity along the Ulysses trajectory. The computed intensities are simply one steady-state solution plotted with the Ulysses position as the only time varying entity.

For the Jovian electrons only (third panel), it follows that for the simulated period 1994 to 1997 when Ulysses moved to higher latitudes the differences between the solutions for different d 's is the largest. The effect of an increasing d causes more Jovian electrons to reach higher latitudes. When Ulysses was in or close to the equatorial plane, from launch up to 1993, and after 1997 up to 1998, there is no noticeable effect in the solutions corresponding to different d 's. This is due to the dominating Jovian source and also that for all d 's, the function $F(\theta) = 1$ in the equatorial regions (see Figure 1).

For the simulated galactic electrons only, (fourth panel), the different assumptions for d resulted in significantly different solutions along the whole Ulysses trajectory. The largest difference occurs when Ulysses moved towards the higher latitudes for the simulated period 1994 up to 1997. In all cases an increase in the galactic electron intensity is found towards higher latitudes but the larger the enhancement of $K_{\perp\theta}$ is towards the poles, the smaller the latitudinal dependence becomes. It is evident from the combined Jovian and galactic electron simulations (fifth panel) that the Jovian source should dominate in the equatorial regions up to the simulated period of 1993 resulting in little to no difference in the solutions for the four assumed values of d . For the simulated period of 1997 up to 1998 Ulysses returned to the equatorial regions, but Jupiter was now on the other side of the Sun. The difference between the solutions for different d 's is larger than for the period from launch up to 1993 indicating that although $F(\theta)$ is only larger at the poles for the four scenarios for d , there is still a difference in the solutions because of the global transport of the galactic electrons from the modulation boundary to the position of Ulysses.

For the simulated periods 1993 to 1997, large differences are found between the four solutions. This indicates the important role that the latitudinal transport

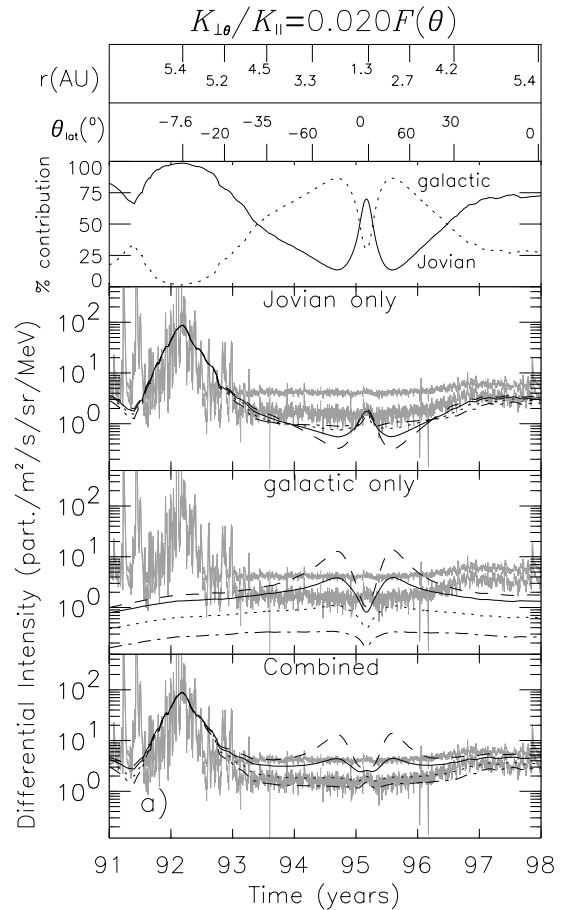


Fig. 2. The first panel shows the radial distance of Ulysses from the Sun (top) and its heliographic latitude, θ_{lat} , (bottom) at selected time periods. Second panel shows the relative contribution of the Jovian (solid line) and galactic (dotted line) electron intensity to the total computed intensity. Third panel shows the computed 7 MeV Jovian electron intensities along the Ulysses trajectory for four assumptions of d in Eq. (6). The dashed line corresponds to solutions produced with $d = 1$, the solid line to $d = 2.5$, the dotted line to $d = 6$, and the dashed-dotted line to $d = 13$. In comparison, the 3-10 MeV electron count rate (described in text) of the COSPIN/KET instrument onboard Ulysses is shown as gray lines. Fourth panel shows the computed 7 MeV galactic intensity only, and the fifth panel the combined Jovian and galactic electron intensity.

coefficient plays in establishing the latitude effects in the inner heliosphere.

To produce compatibility with the electron data at these energies, our results indicate that $K_{\perp\theta}$ should be enhanced by a factor of ~ 2.5 , which comes to $\sim 5\%$ of K_{\parallel} in the polar regions. This may change for a different assumption of b .

Lastly, the Jovian and galactic electrons are separated to show the relative contribution of each of these two populations to the total intensity. The second panel shows the percentage contribution of each electron population to the total intensity with $d = 2.5$. This scenario produces compatibility between the data and model computations up to 1998.

Studying these relative contributions for both scenarios it is found that during the simulated Jupiter encounter, up to

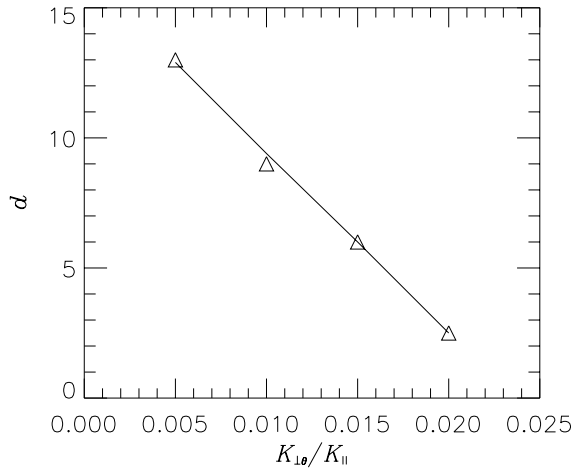


Fig 3. The value of the factor d increase in $K_{\perp\theta}$ towards the poles as a function of the ration $K_{\perp\theta}/K_{\parallel}$ in the equatorial plane as needed to compute solutions compatible with ~ 7 MeV electron observations.

1993, the time-profile is clearly Jovian electron dominated, contributing over $\sim 80\%$ of the total electron intensities. Towards higher latitudes the contribution of the Jovian electrons decreases, while consequently the galactic component increases, resulting in galactic electrons contributing over $\sim 60\%$ up to 1996.5. The exception of course is the fast latitude scan in 1995 when the two contributions reverse. After 1996.5, the large K_{\parallel} in the inner heliosphere resulted in a simulated contribution of Jovian electrons of over $\sim 60\%$ up to 1998, although Jupiter was at the other side of the Sun.

This study was repeated for three other ratios of $K_{\perp\theta}/K_{\parallel}$ (not shown here) in the equatorial plane, namely $b = 0.005$, $b = 0.010$ and $b = 0.015$. It was found that in order to produce compatibility between the model solutions and the observed data from COSPIN/KET onboard Ulysses up to 1998, the values should be $d = 6.0$ for $b = 0.015$, and $d = 9.0$ for $b = 0.010$, and $d = 13.0$ for $b = 0.005$.

These four different scenarios of $K_{\perp\theta}/K_{\parallel}$ and the corresponding d that is needed to produce compatibility with data respectively are plotted in Fig. 3 where d is plotted as a function of $K_{\perp\theta}/K_{\parallel}$ in the equatorial plane. Figure 3 shows a linear dependence between d and $K_{\perp\theta}/K_{\parallel}$ when solutions compatible to 7 MeV electron observations are produced. It can thus be concluded that the ratio $K_{\perp\theta}/K_{\parallel}$ could be as high as $b = 0.020$ and as low as $b = 0.005$ in the equatorial regions at low energies and/or even time dependent as long as the factor d is changed correspondingly as shown in Fig. 3. This indicates that to produce compatibility with data the factor increase in $F(\theta)$ and therefore $K_{\perp\theta}$ towards the poles is dependent on the ratio $K_{\perp\theta}/K_{\parallel}$ in the equatorial plane. Furthermore, Fig. 3 shows an upper limit to the value of $K_{\perp\theta}$ in the polar regions where $K_{\perp\theta}/K_{\parallel}$ is 0.050 - 0.065 for solutions compatible to data.

4. Conclusions

A three dimensional numerical model, including the Jovian source, was used to illustrate the effects of different $K_{\perp\theta}$ on modulation along the Ulysses trajectory. The model results were compared to observed 3-10 MeV electron counting rates measured by the COSPIN/KET detector onboard Ulysses (Ferrando, et al., 1999; Heber et al., 2001). We found that:

1. $K_{\perp\theta}$ plays an important role in determining the Jovian and galactic electron intensities towards the higher heliolatitudes.
2. The ration $K_{\perp\theta}/K_{\parallel}$ could be as high as 0.020 and as low as 0.005 in the equatorial regions at low energies as long as the enhancement factor d is changed correspondingly as shown by Fig. 3.
3. An upper limit of 0.050 to 0.065 for the value of $K_{\perp\theta}$ in the polar regions is proposed.
4. The relative contribution of Jovian and galactic electrons to the total intensity along the Ulysses trajectory could be determined.

Acknowledgements. We thank the South African National Research Foundation (NRF), and the Deutsche Forschungsgemeinschaft (DFG) for financial support.

References

- Bieber, J. W., Matthaeus, W. H., Smith, C. W., Wanner, W., et al., *Astrophys. J.*, **420**, 294, 1994.
- Burger, R. A., Potgieter, M. S., Heber, B., *J. Geophys. Res.*, **105**, 27447, 2000.
- Eraker, J. H., *Astrophys. J.*, **257**, 862, 1982.
- Ferrando, P., Raviart, A., Haasbroek, L. J., Potgieter, M. S., Droge, W., Heber, B., et al., *Astron. Astrophys.*, **316**, 528, 1996.
- Ferrando, P., Raviart, A., Heber, B., Bothmer, V., Kunow, H., et al., *Proc 26th ICRC*, **7**, 135, 1999.
- Ferreira, S. E. S., Potgieter, M. S., Burger, R. A., and Heber, B., *J. Geophys. Res.*, **105**, 18305, 2000.
- Ferreira, S. E. S., Potgieter, M. S., Burger, R. A., Heber, B., and Fichtner, H., *J. Geophys. Res.*, in press, 2001a.
- Ferreira, S. E. S., Potgieter, M. S., Burger, R. A., Heber, B., et al., *J. Geophys. Res.*, submitted, 2001b.
- Heber, B., Ferrando, P., Raviart, A., Paizis, C., et al., *Adv. Space Res.*, in press, 2001.
- Jokipii, J. R., and Kóta, J., *Geophys. Res. Lett.*, **16**, 1, 1989
- Jokipii, J. R., and Kóta, J., *Proc. 24th ICRC*, **4**, 718, 1995
- le Roux, J. A., Zank, G. P., and Ptuskin, V. S., *J. Geophys. Res.*, **104**, 24845, 1999.
- Kóta, J., and Jokipii, J. R., *Proc. 24th ICRC*, **4**, 680, 1995
- Lopate, C., *Proc. 23rd ICRC*, **3**, 415, 1991.
- Langner, U. W., de Jager, O. C., and Potgieter, M. S., *Adv. Space Res.*, in press 2001
- McDonald, F. B., Cline, T. L., and Simnett, J. G., *J. Geophys. Res.*, **77**, 2213, 1972.
- Moses, D., *Astrophys. J.*, **313**, 471, 1987.
- Parker, E. N., *Planet. Space Sci.*, **13**, 9, 1965.
- Potgieter, M. S., *J. Geophys. Res.*, **101**, 24411, 1996.
- Pyle, K.R., and Simpson, J. A., *Astrophys. J. Let.*, **215**, L89, 1977.
- Simpson, J. A., Hamilton, D., Lentz, G., McKibben, R. B., et al., *Science*, **183**, 306, 1974.
- Simpson, J. A., Anglin, D., Balogh, A., Burrows, J R., *Science*, **257**, 1543, 1992.
- Teegarden, B. J., McDonald, F. B., Trainor, J. H., Webber, W. R., and Roelof, E. C., *J. Geophys. Res.*, **79**, 3615, 1974.